JOURNAL OF COATING TECHNOLOGY AND INNOVATION
Jul-Sept 2024, VOL. 2, ISSUE 3, pp. 26-33
https://doi.org/10.61577/jcti.2024.100015

RESEAPRO JOURNALS

ORIGINAL ARTICLE

OPEN ACCESS

Thermal oxidative degradation of fire retardant HDPE based on ammonium polyphosphate, melamine, pentaerythritol and nanoclay

Yu.M. Yevtushenko

Enikolopov Institute of Synthetic Polymer Materials, Russian Academy of Sciences, Moscow, Russian Federation

ABSTRACT

The key components of intumescent compositions (IC) in many cases are the phosphorus compounds in combination with a carbon source, nitrogen heterocycles, and other special additives. We have studied the thermogravimetric behavior of HDPE composition based on ammonium polyphosphate (APP), pentaerythritol (PER), melamine (MEL) and nano clay (OMMT). A mixture of fillers was dispersed in HDPE in a Brabender unit at 190 °C. On the DSC curve, recorded in the air, endothermic melting peaks of HDPE (126.6 °C, ΔH = - 46.5 J / g) and PFA (322.6 °C, ΔH = - 20.4 J / g) were identified, and exothermic peak HDPE (242.9 °C, ΔH = 116.1 J / g). Unlike the pure HDPE sample (thermal degradation temperature of the beginning of 391.7 °C) on the DSC curve of the filled sample with fire retardant thermal degradation is observed around 410 °C and an exothermic peak has multiple characters (sawtooth shape of the low-temperature shoulder), i.e. we can see oscillation output of products of combustion depending on temperature. On the participation of oxygen in the air this process shows corresponding curves DSC and TGA, recorded in an argon atmosphere where the thermal degradation peak is not split. This data suggests that the cause of the oscillating nature of the reaction yield is the thermo-oxidative degradation of fillers. Some assumptions about processes were discussed.

KEYWORDS

Intumescent systems; High-density polyethylene (HDPE); Oscillation output

ARTICLE HISTORY

Received 26 August 2024; Revised 23 September 2024; Accepted 30 September 2024

Introduction

Synthetic polymers and composites are important materials in modern industry and technology. Now synthetic polymers are rapidly replacing metals, concrete etc. However, the main disadvantage of polymers is that these materials are combustible under certain conditions. Therefore, it is very important to decrease the combustion of polymers. It can be done by two main methods: (1) to protect the surface of polymers from fire [1-5]; (2) to add fireproofing substances in the bulk of polymers [6-10]. There are some substances which can be used in both cases. The compositions on the base of ammonium polyphosphate (APP), pentaerythritol (PER) and melamine (MEL) are the most common to increase the fireproofing properties special additives are used (TiO_2, boric acid, nano clays and some other fillers) [11].

The invention [12] relates to a flame retardant article comprising a polyolefin substrate, a specific phosphonate ester, and a synergist comprising an N-alkoxy hindered amine and melamine cyanurate. Another aspect of the invention is the flame retardant composition itself and the use thereof to increase the flame retardancy of polyolefins. It also relates to flame retardant compositions comparing a specific phosphonate ester and a specific non-triazine containing N-alkoxy hindered amine.

A polyolefin substrate with additives incorporated therein is described [13]. The additives consist of an organophosphorus compound including a phosphonate ester, a phosphate ester, or a combination thereof; and a synergist including an N-alkoxy hindered amine. A performance rating of the article from a UL-94 vertical burn (VB) test achieves a V-0 rating when the article is in the form of a 125-mil injection molded bar.

S. Rabe et al, incorporated phosphorus-based flame retardants into different polymeric thermoset resins and paraffin as a proposed model for polyolefins and investigated their flame retardant performance [14]. The favored mode of action of each flame retardant sample was identified in each respective system and at each respective concentration. Thermogravimetric analysis was used in combination with infrared spectroscopy of the evolved gas to determine the pyrolysis behavior, residue formation and the release of phosphorus species. Forced flaming tests in the cone calorimeter provided insight into burning behavior and macroscopic residue effects. The results were put into relation to the phosphorus content to reveal correlations between phosphorus concentration in the gas phase and flame inhibition performance, as well as phosphorus concentration in the residue and condensed phase activity. Total heat evolved (fire load) and peak heat release rate were calculated based on changes in the effective heat of combustion and residue, and then compared with the measured values to address the modes of action of the flame retardants quantitatively. The quantification of flame inhibition, charring, and the protective layer effect measure the non-linear flame retardant effects as functions of the phosphorus concentration. Overall, this screening approach using easily prepared polymer systems provides great insight into the effect of phosphorus in different flame retarded polymers, concerning polymer structure, phosphorus concentration, and phosphorus species.

***Correspondence:** Dr. Yu.M. Yevtushenko, Enikolopov Institute of Synthetic Polymer Materials, Russian Academy of Sciences, Moscow, Russian Federation, email: evt-yuri@mail.ru

Radiation shielding materials should have high thermal stability and environmental resistance. In the study [15], attempts were made to develop a polymeric material using High-Density Polyethylene (HDPE) via imparting flame retardant characteristics as well as neutron shielding by the addition of ammonium dihydrogen phosphate ($NH_4H_2PO_4$)/silicon dioxide (SiO_2) mixtures of different compositions with fixed portions of lead oxide Pb_2O_3. Flame retardant properties as well as the thermal stability of the developed composite materials evaluated by studying the burning behavior test, the Limiting Oxygen Index (LOI), and thermogravimetric analysis (TGA) as a function of ($NH_4H_2PO_4/SiO_2$) percentage. Results show that the flame retardant performance and thermal stability of the composite materials were improved as a result of the inclusion of ($NH_4H_2PO_4/SiO_2$) and such improvement increases by increasing the additive portion. The obtained results also indicated that exposure to a 30 kg. irradiation dose has no significant effect on the mechanical properties of the developed material.

There are some other combinations of different substances, but it is very important to substitute traditional very dangerous halogen- and antimony-containing compounds [16, 17]. This paper reports on the effect that the proper combination of APP, PER, MEL and nano clay can be used to decrease PE flammability.

Experimental

We used ammonium polyphosphate APP-1 (Phase II) n> 1500 (NPF "Tehnohim"), pentaerythritol PER (GOST 9286-89), melamine MEL (GOST 7579-76) and nano organoclay “Dellite 72t”, Laviosa, Italy (MMT) as a complex fire retardant and high-density polyethylene (HDPE). A mixture of fillers (28-35%) dispersed in HDPE (65-72%) mixed to a Brabender at 190 °C (PNCPE). Test specimens were prepared by pressing at 180 °C. As a comparison, we used a fire-retardant PE (ZBPPE) sample with Zn-B-P-containing fire retardants according to the elemental analysis. Both samples correspond to the classification of V_o UL 94V Underwriters Laboratories standard.

(Table 1) presents the results of the study of the optimal ratio of different components in the composite material according to test procedure UL 94. There are three samples (No. 23-25) that correspond to the flammability rating V_o standard UL 94 after two fire applications. Sample No. 23 obtains the best properties according to UL 94 - total burning time after 10 flame applications is 34 s and burning and afterglow times after second flame application is 18 s.

Table 1. Sample composition and test results according to UL 94.

№	Components, g						Burning time, (c) No. application		Drops	UL 94
	PE	APP	MEL	PER	MMT	Additives, g	1	2		
1	74.5	12.0	12.0	-	1.5	-	2	>10	-	-
2	70.0	15.0	15.0	-	-	-	>10	-	-	-
3	74.5	14.0	14.0	-	1.5	-	2	15	-	-
4	88.5	6.5	3.0	-	1.5	-	2	>10	-	-
5	83.5	11.0	5.0	-	1.5	-	2	>10	-	-
6	78.5	14.0	6.0	-	1.5	-	1	>10	-	-
7	68.5	20.0	10.0	-	1.5	-	1	>10	-	-
8	73.5	14.0	6.0	5.0	1.5	-	2	>10	-	-
9	75.5	14.0	6.0	-	1.5	ATH 5.0	1	>10	-	-
10	81.5	10.0	3,3	3,3	2.0	-	2	>10	-	-
11	80.5	9.0	6.0	6.0	2.0	-	2	>10	+	-
12	78.0	11.0	2.0	7.0	2.0	-	2	>10	+	-
13	75.0	12.5	4,2	8,3	2.0	-	1	3	+	HB
14	75.0	12.5	3.0	6,3	2.0	-	2	>10	+	-
15	75.0	19.0	6.3	-	2.0	-	2	6	-	HB
16	75.0	16.0	9.0	-	2.0	-	1	2	+	HB
17	75.0	12.4	4.2	8,4	2.0	-	2	>10	-	-
18	73.0	13,5	4.5	9.0	2.0	-	2	>10	-	-
19	74.3	12.3	4.2	8,3	2.0	HQ 0.9	2	>10	-	-
20	75.0	12.4	-	8.4	2.0	DCDA 4.2	2	>10		-
21	75.0	12.4	4.2	6.0	2.0	ATH 2.4	>10	-	+	-
22	75.0	12.4	-	6.0	2.0	DCDA 4.2	>10	-	+	-
23	68.7	14.7	4.9	9.8	2.0	-	1	4	-	V_0
24	68.7	14.7	-	9.8	2.0	DCDA 4.9	1	8	-	V_0
25	68.7	14.7	-	9.8	2.0	CMEL 4.9	1	2	-	V_0

https://doi.org/10.61577/jcti.2024.100015

DSC and TGA curves were recorded on the device STA 449F3 Jupiter firm NETZSCH. Heating rate 10 K/min. X-ray photoelectron spectra (XPS) were recorded on the UHV analytical unit of electron-ion spectroscopy (EIS) based on NANOFAB 25, X-ray source SPECS X-ray Source XR 50 Al/Mg (1486,6 eV / 1253.6 eV) with dual anode. IR spectra were recorded on NICOLET iS50 FT-IR.

Results and Discussion

According to the thermal analyses data (Figure 1) thermal oxidative degradation of pure HDPE in the ear, used in this work, is characterized by three major peaks in the DSC curve at 130.4 °C (endothermic peak), 243.3 °C and 403.5 °C (exothermic peaks) that generally consistent with published data. Thermal oxidative degradation starts at 391.7 °C and is accompanied by a sharp increase in the exothermic effect (ΔH = 3,39 kJ/g). Residual weight at 600 °C is about 3%.

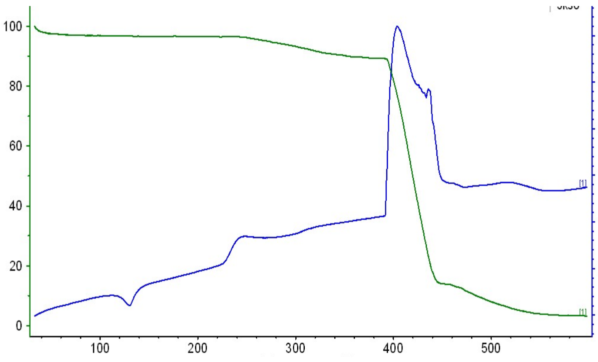

Figure 1. TGA and DSC curves of HDPE.

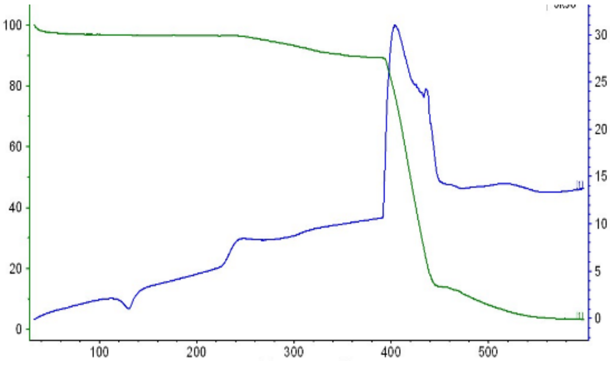

Figure 2. TGA and DSC curves of ZBPPE.

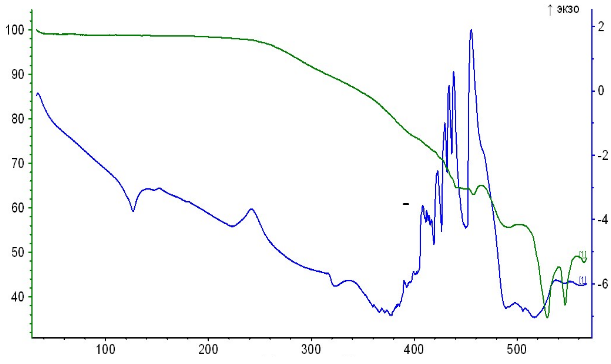

Figure 3. TGA and DSC curves of PNCPE.

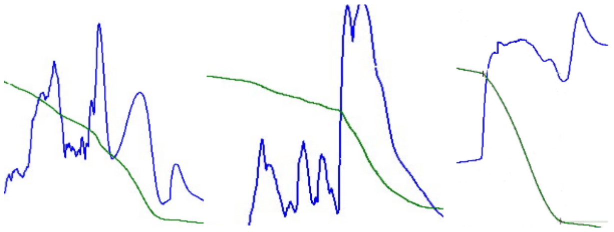

Figure 4. Different characters of TGA and DSC curves of PNCPE.

ZBPPE sample (Figure 2) according to the thermal analysis data is the composition on the base of HDPE (peaks at 125.0 and 250.5 °C). Unlike pure HDPE on the DSC curve of fire-retardant HDPE there are two exothermic peaks (385.5 and 471.2 °C). The first peak is related to the thermal degradation of the flame retardant additive, and the second to the thermal degradation of HDPE.

On the DSC curve of PNCPE (Figure 3), there are three peaks (126.6, 242,9 and 455,4 °C) corresponding to HDPE, and 322,6 °C, corresponding to APP. As a result of the introduction of a fire-retardant additive, the beginning of thermal degradation of HDPE is shifted to the high-temperature region for 65 °C, and the thermal oxidative degradation peak is split into many stripes. The splitting of the DSC curve of the same sample may proceed in different ways (Figure 4). The number of the stripes and the distances between them on the DSC curve may be different and absent at all and depend on the distribution of solid components in IC.

To assess the combustibility of ZBPPE and PNCPE Vertical Burning Test UL 94V was used. It is established that both samples meet the requirements of UL 94 V_o (burning time after first ignition is less than 1 c (Samples 1 and 2), the burning time after second ignition is 5 and 2 c respectively, glow time after the second ignition is 3-4 c (ZBPPE and PNCPE), dropping of the melt is not observed.

In accordance with the data of TGA and DSC the nature of the thermal oxidative degradation of PNCPE and ZBPPE in the air is fundamentally different. The first is the behavior of samples at high temperatures. The weight loss of samples when heated to 600 °C is 50% (PNCPE) and 90% (ZBPPE). Burnt samples (UL 94 V test) showed that on the surface of the PNCPE, a rather thick layer of char is formed, whereas the ZBPPE forms a very thin layer of char. The thermal degradation of the samples in argon is less different: the similar main mass loss of the two samples at 400-480 °C is observed, but when heated to 600 °C the mass loss is 11% (ZBPPE) and 22% (PNCPE). The reason for these differences is due to the different interactions of the samples with oxygen and the different content of fire retardants.

According to the XPS element analyses the composition of the ZBPPE surface is O_{1s} (534.6 eV, 11.8%), C_{1s} (eV 287.6, 83.2%), N_{1s} (402.6 eV, 5.0%), which indicates the presence of a nitrogen-containing flame retardant component, e.g., melamine or derivatives thereof (Figure 5). Elemental analyses of the inner layer of the char are O_{1s} (532.6 eV, 26.2%), C_{1s} (284.6 eV, 47.6%), N_{1s} (401.6 eV, 3.2%), P_{2P} (133.6 eV, 9.3%), B_{1s} (191.6 eV, 13.4%), Zn_{2P} (1022.6 eV, 0.3%) and shows complex composition of matrix (Figure 6). It may be concluded that the fire retardants

https://doi.org/10.61577/jcti.2024.100015

mainly are situated inside the sample and preferably influence the combustion of the condensed phase.

The element analyses of the PNCPE inner layer of the char [O_{1s} (532.5 eV, 7.5%), C_{1s} (eV 285.0, 89.0%), N_{1s} (399.0 eV, 5.0%), P_{2P} (135.0 eV, 1.1%)] reflects that this element mainly consists of carbon derivatives (Figure 7). According to the XPS line C_{1s} (Figure 8), the main component of the inner layer of the char is amorphous carbon. In the XPS of the outer layer of the chare (Figure 9) the lines of all peaks are shifted to the higher bonds' energy [O_{1s} (534.5 eV, 29.7%), C_{1s} (eV 287.5, 57.8%), N_{1s} (399.0 eV, 7.1%), P_{2P} (135.0 eV, 5.2%)] (Figure 10). It can be seen that the C-content of the outer layer of the PNCPE char is significantly lower than the C-content in the inner layer because the equilibrium of the reaction $2CO \leftrightarrow C + CO_2$ at higher temperature on the surface than that in inner layers of the burning sample is shifted to produce carbon monoxide. The higher bond energies of all elements the more thermosetting combination as a result of the sample decomposition.

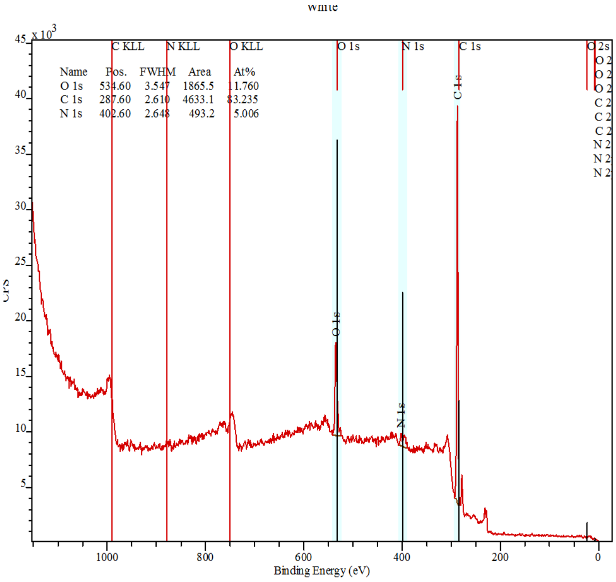

Figure 5. XPS spectra of ZBPPE.

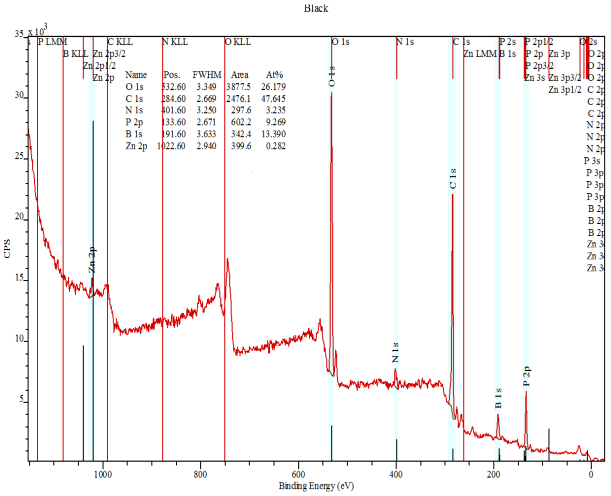

Figure 6. XPS spectra of the ZBPPE inner layer of the char.

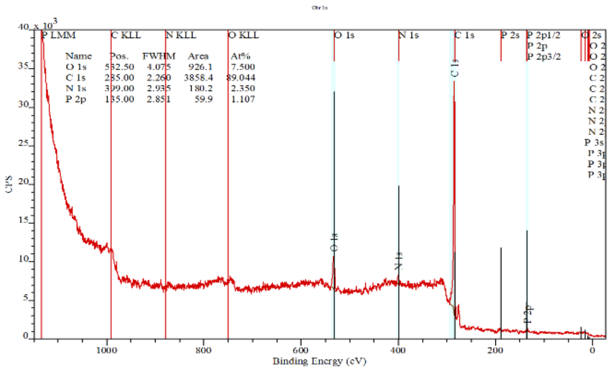

Figure 7. XPS spectra of the PNCPE inner layer of the char.

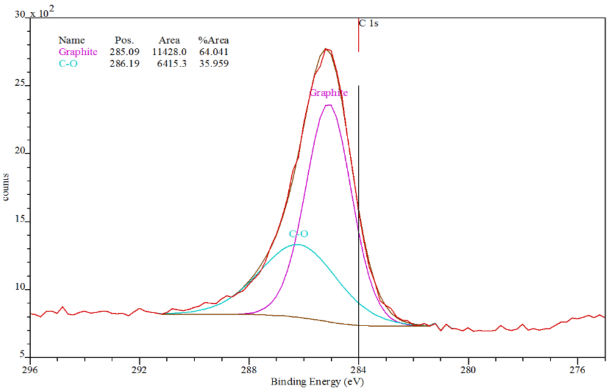

Figure 8. XPS C1s line of the PNCPE inner layer of the chare

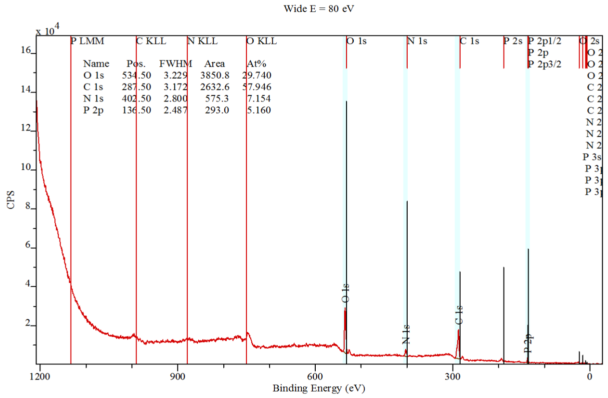

Figure 9. XPS spectra of the PNCPE outer layer of the char.

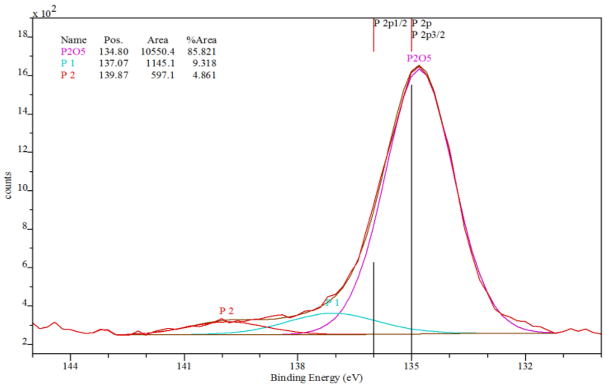

Figure 10. XPS P_{2P} line of the PNCPE inner layer of the chare.

https://doi.org/10.61577/jcti.2024.100015

In the IR spectra of the APP (Figure 11) and PER (Figure 12), there are a number of narrow characteristic absorption bands. The assignment of the bands is represented in [18]. IR spectra of APP show peaks corresponding to phosphate: at about 1250 cm^{-1} for P=O bonds and 1010 and 1070 cm^{-1} for P-O bonds. As a result of heat treatment of APP at 600 °C, there are only three wide complex bands in the IR spectra. In the spectra of the internal (Figure 13) and external (Figure 14) layers of the charge, there are wide absorption bands, which indicates a mixture of products of thermal decomposition of the different structures. First of all, this is due to the formation of several different phosphorus oxides, in the IR spectra of which the frequencies of the absorption bands P-O, P=O and P-H are close, and the broadening of the absorption bands is observed as a result of their overlap [19]. According to elemental analysis, the presence of a significant amount of nitrogen in the outer layer of the chart indicates the possibility of the formation of phosphorus (poly) oxynitrides, the absorption bands of which are present in the region of oscillations of P = O bonds.

There is an absorption band at 1400 cm^{-1} in the IR spectrum of the inner layer of PNCPE foam. In the APP and PER spectra, the nearby bands are detected at 1434 cm^{-1} (APP) and three absorption bands at 1452, 1408, and 1382 cm^{-1} (PER). The wide absorption band at 1434 cm^{-1} is attributed to the vibration of the ammonium salt, which is confirmed by the presence of a wide absorption band in the region of 3300-3100 cm^{-1} (V_{NH}). The absorption bands of PER are related to the valence oscillations of methylene groups and after thermal destruction should be absent in the spectra of the char. The authors [19] believe that the presence of the band 1400 cm^{-1} in the spectrum of the inner layer of PNCPE is due to the presence of the P=O stretch bond. Structures of the P_4O_{6-10} oxides have been determined by electron diffraction and X-ray investigations and these molecules have the same basic structure with four P atoms connected by six bridging O atoms to form an adamantane-like cage and one, two, three, or four additional O atoms in terminal positions on the pentavalent phosphorus atoms.

Assignment of the band at 1400 cm^{-1} to the vibration of ammonium salt is unlikely due to the thermal degradation of APP with the release of ammonia at a temperature below 300 °C. A decrease in the intensity of the absorption band at 1400 cm^{-1} in the spectrum of the outer layer compared to the inner one is accompanied by a shift of the absorption band of the inner layer at 1271 cm^{-1} ($\nu_{P=O}$) to the high-frequency region at 1313 cm^{-1}. The isotopic shifts of the P=O stretching vibrations give evidence for some coupling to cage motions and between the P=O stretching vibrations across the P-0-P bridges. The presence of doublets at 1400-1300 and 1000-900 cm^{-1} in the spectra of the outer and inner layers of PNCPE is a characteristic property of phosphorus compounds due to the possibility of rotation isomerism [20].

The spectra of different combinations of reagents (Figures 12-16) after heating to 600 °C are different (Table 2). This means that the number of end products and their mass fraction depends on both the ratio of the initial products and the temperature-time mode of heat treatment.

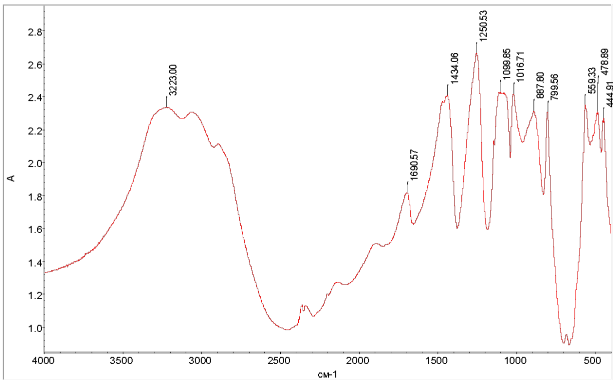

Figure 11. The IR spectrum of APP.

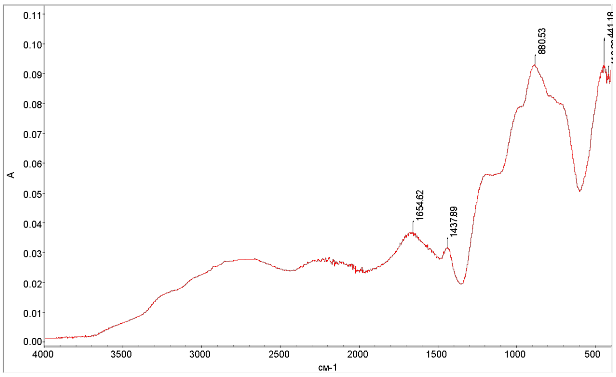

Figure 12. IR spectrum of APP after heating at 600 °C.

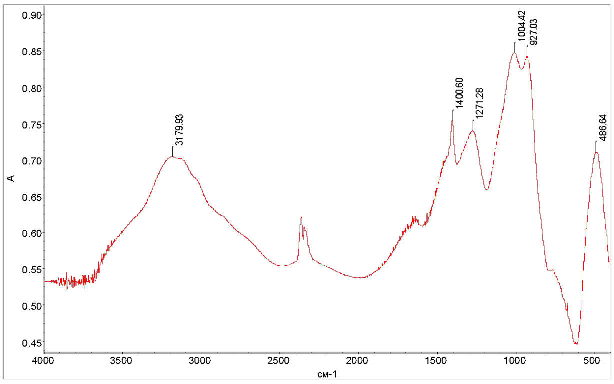

Figure 13. IR spectrum of PNCPE after heating at 600 °C (inner layer).

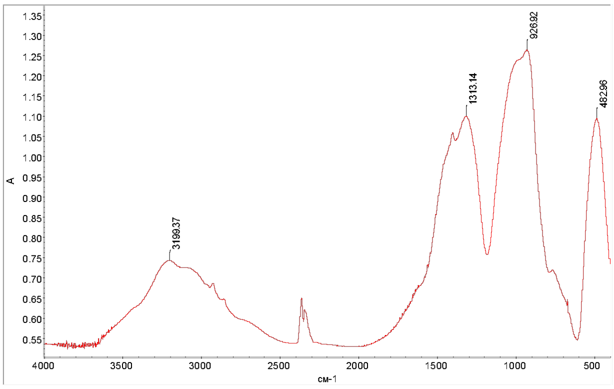

Figure 14. IR spectrum of PNCPE after heating at 600 °C (outer layer).

https://doi.org/10.61577/jcti.2024.100015

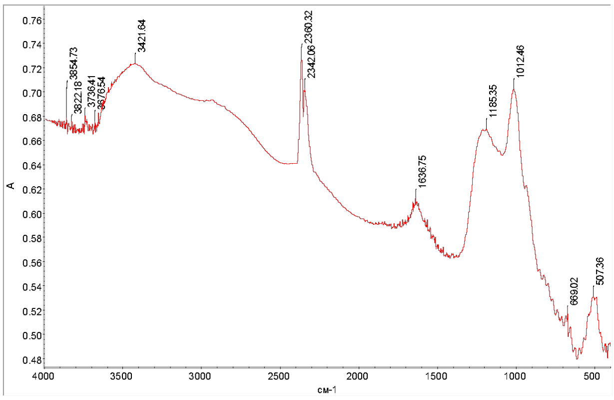

Figure 15. IR spectrum of APP+PER after heating at 600 °C.

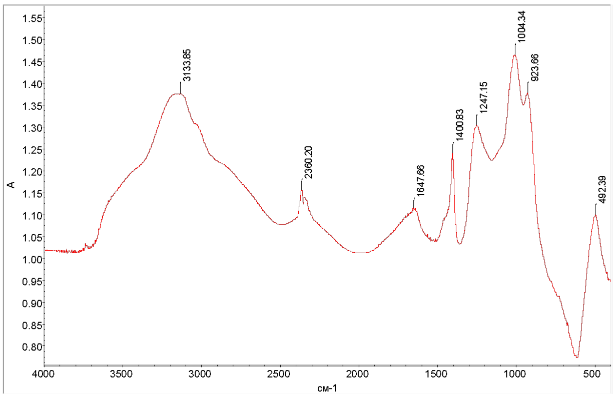

Figure 16. IR spectrum of APP+MEL after heating at 600 °C.

Table 2. Observed Vibrational Frequencies (cm-') for 11-16 spectra.

Figure	P=O stretch	P=O, P=N	P-O, P-N, P-O-P	P=O bending	P_4O_6
11	1434	1260	1004, 887	559	478, 445
12	1437	Shoulder	880	-	441
13	1400	1271	927	-	486
14	Shoulder	1313	Doublet 926	-	492
15	-	1185	Doublet 1012	-	507
16	1400	1247	1004, 923	-	492

Fire retardant composition PNCPE can be considered as a special case of intumescent coating including binder (PE), acid source (APP), source of carbon (PER) and blowing agent (MEL). Therefore, the formation of the char on the surface of PNCPE is the main reason for the fire resistance of composite materials of this type and can be represented in the form of the diagram (Figure 17).

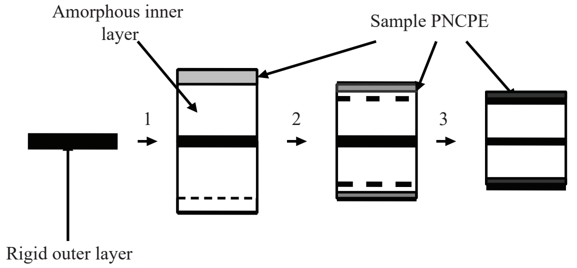

Figure 17. Char formation diagram on the surface of PNCPE.

The chare formation according to scheme 17 begins at 300-320 °C (stage 1). This chare consists of two layers – the thick inner layer of amorphous type and a more rigid thin outer layer due to the formation of a small mass fraction of ceramics similar to the base of O-P-N bonds. As a result, the penetration of oxygen and heat to the substrate becomes lower and the emission of gaseous combustible products decreases. Decomposition of PNCPE proceeds slowly and as the temperature increases, the carbon content in the outer layer decreases due to the $C + CO_2 \rightarrow 2CO$ reaction [14] and this barrier becomes rather weak (stages 2-3). Penetration of heat and oxygen into the char is increased and the cycle of formation and destruction of the external layer of the char is repeated. So, the thermal distraction of PNCPE can be represented by multiple peaks on the DSC curves. Such oscillations are irregular and may be absent at all (Figure 4). As a result, there are several waves on the surface of the char in the case of oscillated formation (Figure 18 a) and without waves when no oscillation (Figure 18 b). The formation of an amorphous thick layer of the char occurs due to the reaction of APP and PER, while the outer strong layer of the char is formed as a result of the reaction of APP and MEL (Figure 19).

The polymer pyrolysis is the key step in polymer combustion, the chemical process producing the fuel that feeds the flame according to the fire loop. When this cyclic process is interrupted at any point, the combustion stops and resumes if the cycle is restored. We may propose that the char formation without oscillation is possible due to the absence of a weak outer layer and this process is presented in (Figure 20).

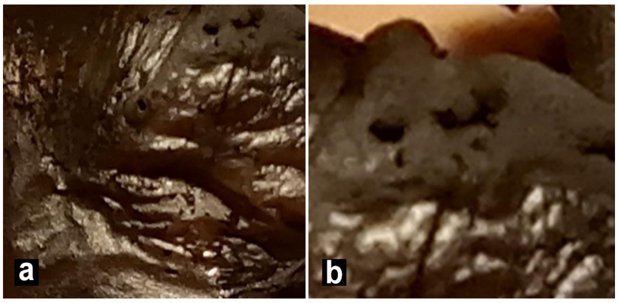

Figure 18. The surface of the char produced in oscillation mode (a) and without oscillation(b)

https://doi.org/10.61577/jcti.2024.100015

Figure 19. The amorphous thick layer of the char after the reaction of APP and PER (left) and the outer thin rigid layer of the char after the reaction of APP and MEL (right) at the temperature 600 °C.

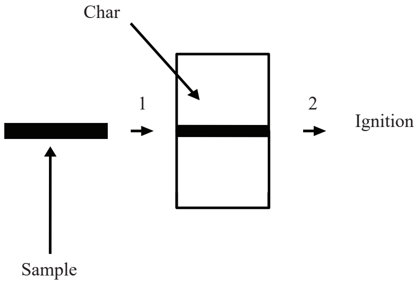

Figure 20. The formation of the char on the surface of fire-retardant composite materials based on PE in oscillating mode is of interest in practical terms.

The DSC curves in the PNCPE thermos destruction region are represented as discrete peaks. Temperature regions with minimal heat release are bifurcation points. Upon reaching the appropriate temperature combustion of composite material slows or stops. With further increase of temperature or prolonged exposure at this temperature, combustion is resumed. The discrete nature of the combustion of fire-retardant composite materials makes it possible to slow down or stop the combustion at various stages of thermal destruction, corresponding to the temperatures of the bifurcation points.

Conclusions

The results of a study of two typical methods of char formation and functional properties during oxidative thermal degradation are presented. It is shown that using a mixture of APP, PER and MEL oxidative process occurs in an oscillating mode. It is assumed that in the temperature range of 400–460 °C by a vented heat source, the combustion of the specimen ceases due to the formation of char, which consists of the outer solid layer (a mixture of ceramics similar to phosphorus oxo nitrides and amorphous carbon). It has proven synergistic effects of phosphorus and nitrogen-containing flame retardants. With further increase in temperature of the outer source solid layer is enriched with oxo nitrides due to the decrease in the proportion of amorphous carbon and prevents further thermal oxidative degradation of PE up to 600 °C. The presented findings should be seen as a special case for reducing the combustibility of PE.

Acknowledgement

The work was carried out with the participation of employees of the Center for Collective Use of ISPM RAS within the framework of the research work "Development of new types of high-tech polymer and composite materials with a complex of special properties based on flexible and rigid-chain polymers of various natures using new principles and theoretical approaches for various fields of industrial production, construction and medicine" (FFSM-2024-0002). The author would like to thank I.O. Kuchkina and A.N. Ozerin for their assistance during the experimental testing.

Disclosure Statement

No potential conflict of interest was reported by the authors.

References

1. Mohd Sabee MM, Itam Z, Beddu S, Zahari NM, Mohd Kamal NL, Mohamad D, et al. Flame-retardant coatings: additives, binders, and fillers. Polymers. 2022;14(14):2911. https://doi.org/10.3390/polym14142911
2. Dreyer JA, Weinell CE, Dam-Johansen K, Kiil S. Review of heat exposure equipment and in-situ characterisation techniques for intumescent coatings. Fire Saf J. 2021;121:103264. https://doi.org/10.1016/j.firesaf.2020.103264
3. Li GQ, Han J, Wang YC. Constant effective thermal conductivity of intumescent coatings: Analysis of experimental results. J Fire Sci. 2017;35(2):132-155. https://doi.org/10.1177/0734904117693857
4. Li Y, Cao CF, Chen ZY, Liu SC, Bae J, Tang LC. Waterborne Intumescent Fire-Retardant Polymer Composite Coatings: A Review. Polymers. 2024;16(16):2353. https://doi.org/10.3390/polym16162353
5. Markert F, González I, Rogero CD, Hosta ES. Protection of pre-treated wood and construction materials using intumescent coatings. J Phys Conf Ser. IOP Publishing. 2023;2654(1):012084. https://doi.org/10.1088/1742-6596/2654/1/012084
6. Kamalipour J, Beheshty MH, Zohuriaan-Mehr MJ. Flame retardant compounds for epoxy resins: A review. Iran J Polym Sci Technol. 2021;34(1):3-27. https://doi.org/10.22063/JIPST.2021.1790
7. Bifulco A, Varganici CD, Rosu L, Mustata F, Rosu D, Gaan S. Recent advances in flame retardant epoxy systems containing non-reactive DOPO based phosphorus additives. Polym Degrad Stab. 2022;200: 109962. https://doi.org/10.1016/j.polymdegradstab.2022.109962
8. Mensah RA, Shanmugam V, Narayanan S, Renner JS, Babu K, Neisiany RE, et al. A review of sustainable and environment-friendly flame retardants used in plastics. Polym Test. 2022;108: 107511. https://doi.org/10.1016/j.polymertesting.2022.107511
9. Battig A, Markwart JC, Wurm FR, Schartel B. Hyperbranched phosphorus flame retardants: Multifunctional additives for epoxy resins. Polym Chem. 2019;10(31):4346-4358. https://doi.org/10.1039/C9PY00737G
10. Liu C, Zhang P, Shi Y, Rao X, Cai S, Fu L, et al. Enhanced fire safety of rigid polyurethane foam via synergistic effect of phosphorus/nitrogen compounds and expandable graphite. Molecules. 2020;25(20):4741. https://doi.org/10.3390/molecules25204741
11. Wang F, Liao J, Yan L, Cai M. Facile construction of polypyrrole microencapsulated melamine-coated ammonium polyphosphate to simultaneously reduce flammability and smoke release of epoxy resin. Polymers. 2022;14(12):2375. https://doi.org/10.3390/polym14122375
12. Yargici Kovanci C, Nofar M, Ghanbari A. Synergistic enhancement of flame retardancy behavior of glass-fiber reinforced polylactide composites through using phosphorus-based flame retardants and chain modifiers. Polymers. 2022;14(23):5324. https://doi.org/10.3390/polym14235324
13. Helmy M, Ullmann J, Adner D, Otto T, Schadewald A. The effect of the presence of a macromolecular organophosphorus flame

https://doi.org/10.61577/jcti.2024.100015

retardant, poly (N-[3-oxopropylmethylphosphinate] ethyleneimine), on the flammability, thermal stability, and mechanical properties of polyamides. Fire Mater. 2022;47(2):241-250. https://doi.org/10.1002/fam.3092

14. Rabe S, Chuenban Y, Schartel B. Exploring the modes of action of phosphorus-based flame retardants in polymeric systems. Materials. 2017;10(5):455. https://doi.org/10.3390/ma10050455
15. Salem EF, Khozemy EE, Ali AE. Potential flame retardancy of high-density polyethylene (HDPE) composite for possible use as a radiation shield. Prog Nucl Energy. 2023;165:104900. https://doi.org/10.1016/j.pnucene.2023.104900
16. Lucherini A, Maluk C. Intumescent coatings used for the fire-safe design of steel structures: A review. J Constr Steel Res. 2019;162:105712. https://doi.org/10.1016/j.jcsr.2019.105712
17. Li FF. Comprehensive review of recent research advances on flame-retardant coatings for building materials: Chemical ingredients, micromorphology, and processing techniques. Molecules. 2023;28(4):1842. https://doi.org/10.3390/molecules28041842
18. Evtushenko YM, Grigoriev YA, Rudakova TA, Ozerin AN. Effect of aluminum hydroxide on the fireproofing properties of ammonium polyphosphate–pentaerythritol-based intumescent coating. J Coat Technol Res. 2019;16:1389-1398. https://doi.org/10.1007/s11998-019-00221-6
19. Weiss S, Seidl R, Kessler W, Kessler RW, Zikulnig-Rusch EM, Kandelbauer A. Unravelling the phases of melamine formaldehyde resin cure by infrared spectroscopy (FTIR) and multivariate curve resolution (MCR). Polymers. 2020;12(11):2569. https://doi.org/10.3390/polym12112569
20. Camino B, Camino G. The chemical kinetics of the polymer combustion allows for inherent fire retardant synergism. Polym Degrad Stab. 2019;160:142-147. https://doi.org/10.1016/j.polymdegradstab.2018.12.018

https://doi.org/10.61577/jcti.2024.100015